



The top-to-the-southeast Sarzeau shear zone and its place in the late-orogenic extensional tectonics of southern Armorica

Paul Turrillot, Romain Augier, Michel Faure

► To cite this version:

Paul Turrillot, Romain Augier, Michel Faure. The top-to-the-southeast Sarzeau shear zone and its place in the late-orogenic extensional tectonics of southern Armorica. *Bulletin de la Société Géologique de France*, 2009, 180 (3), pp.247-261. 10.2113/gssgbull.180.3.247 . insu-00411234

HAL Id: insu-00411234

<https://insu.hal.science/insu-00411234>

Submitted on 3 Sep 2010

HAL is a multi-disciplinary open access archive for the deposit and dissemination of scientific research documents, whether they are published or not. The documents may come from teaching and research institutions in France or abroad, or from public or private research centers.

L'archive ouverte pluridisciplinaire **HAL**, est destinée au dépôt et à la diffusion de documents scientifiques de niveau recherche, publiés ou non, émanant des établissements d'enseignement et de recherche français ou étrangers, des laboratoires publics ou privés.

The top-to-the-Southeast Sarzeau Shear Zone and its place in the late-orogenic extensional tectonics of Southern Armorica

Paul Turrillot^{1,2}, Romain Augier¹, Michel Faure¹

(1) Institut des Sciences de la Terre d'Orléans (ISTO), UMR CNRS 6113, 45067 Orléans cedex 2, France

(2) Bureau de Recherches Géologiques et Minières (BRGM), GEO G2R, BP 36009, 45060 Orléans Cedex 2, France.

Paul Turrillot, addresses mail: p.turrillot@brgm.fr ou paul.turrillot@univ-orleans.fr

Key words. - Late-orogenic extension, extensional shear-zone, monazite U-Th/Pb chemical dating, Armorican Massif, Variscan Belt

Abstract. - This study presents new structural and monazite chemical U-Th/Pb geochronological constraints for the magmatic rocks of the Golfe du Morbihan area, in Southern Brittany, south of the South Armorian Shear Zone (SASZ). A major extensional shear zone, defined here as the “Sarzeau Shear Zone” (SSZ), separates Carboniferous migmatites and the St-Anne d'Auray type anatetic granite from highly retrogressed micaschists in its footwall and hangingwall, respectively. Late Carboniferous leucogranite dykes, called the Sarzeau granite that intrude the Lower Unit are progressively sheared and mylonitised within the SSZ. The SSZ is characterised by a low to moderately SE-dipping foliation and a NW-SE trending stretching lineation. Kinematic criteria indicate a top-to-the-SE sense of shear. Below the SSZ, NNE-SSW-trending, leucogranitic dykes sometimes present a wall-parallel magmatic layering. These dykes that intrude into vertical NW-SE trending migmatites are interpreted here as emplaced as tension gashes, whose direction opening is consistent with the NW-SE regional stretching. The 316-321 Ma U-Th/Pb ages

yielded by the monazite in the dykes comply with the interpretation of a synkinematic magmatism. In the Golfe du Morbihan, the geometric relationships between the SSZ and the migmatitic host rocks do not support a previous interpretation as a Metamorphic Core Complex. Regionally, the SSZ kinematics is consistent with the Late Carboniferous orogen-parallel extension, already recognised in other areas of Southern Armorica, but does not support the 200km –long flat detachment fault model.

La zone de cisaillement ductile vers l'Est de Sarzeau et sa place dans la tectonique tardi-orogénique extensive de l'Armorique méridionale

Mots clés.- Extension tardi-orogénique, zone de cisaillement extensive, datation chimique U-Th/Pb sur Monazite, Massif Armoricain, Chaîne Varisque

Résumé.- Cette étude apporte de nouvelles contraintes structurales et géochronologiques (méthode chimique) U-Th/Pb pour les roches magmatiques de la zone du Golfe du Morbihan situé en Armorique méridionale, et plus précisément au sud du Cisaillement Sud Armoricain (CSA). Une structure ductile extensive majeure définie ici comme la Zone de Cisaillement de Sarzeau (ZCS), constitue la limite entre deux unités de degrés métamorphiques différents. L'unité inférieure est constituée de migmatites et du granite d'anatexie de S^{te}-Anne d'Auray daté du Carbonifère, alors que l'unité supérieure est constituée de micaschistes fortement rétromorphosés. L'unité inférieure est recoupée à angle droit par des filons de leucogranite datés ici du Carbonifère supérieur. Ces filons sont progressivement cisaillés par le jeu de la ZCS. Cette dernière est caractérisée par une foliation mylonitique à faible pendage vers le SE et une linéation d'étirement orientée NW-SE. Les critères cinématiques indiquent un cisaillement vers le SE. Dans l'unité inférieure, des filons de leucogranite orientés

préférentiellement NNE-SSW montrent parfois une foliation magmatique parallèle aux épontes. Ils s'injectent dans un encaissant migmatitique caractérisé par une foliation verticale orientée NW-SE, et sont interprétés comme le remplissage de fentes de tension dont l'ouverture serait directement due à l'étirement régional également responsable du mouvement extensif de la ZCS. Les âges chimiques U-Th/Pb sur monazite compris entre 316-321Ma obtenus sur des monazites provenant des filons leucogranitiques corroborent l'hypothèse d'un magmatisme syn-tectonique. Dans le Golfe du Morbihan, les relations géométriques entre la ZCS et la foliation verticale des migmatites encaissantes remettent en question l'hypothèse d'un modèle de Metamorphic Core Complexe extensif précédemment proposé pour cette zone. A l'échelle régionale, la cinématique vers le SE de la ZCS est en accord avec une extension Carbonifère parallèle à l'orogène admise pour le domaine Sud Armoricain mais ne s'accorde pas avec l'existence d'une unique zone de détachement plat de 200km de long.

INTRODUCTION

It is widely acknowledged that in collisional orogens, the thickened continental crust commonly experiences thinning driven by gravitational instability. Removal of the thick orogenic root is thus accommodated by normal faulting coeval with the opening of intramontane sedimentary basins and by partial melting. Such a process has been documented in the French Variscan belt. In the French Central Massif, several ductile normal faults, metamorphic domes and syn-kinematic plutons are described [e.g. Malavielle *et al.*, 1990; Van Den Driesche and Brun, 1991-92; Faure, 1995 and enclosed references]. Numerous studies have demonstrated the relationships between pluton emplacement and the regional extensional setting [e.g. Faure and Pons, 1991; Roig *et al.* 1998; Talbot *et al.*, 2005; Joly *et al.*, 2007]. Deformation-assisted thinning mechanisms have been also invoked in the southern part of the Armorican Massif [Gapais *et al.*, 1993; Brown and Dallmeyer, 1996; Cagnard *et*

al., 2004] that presents numerous lithological and structural similarities with the Central Massif. South of Vannes, migmatites and peraluminous granitoids are well exposed along the Golfe du Morbihan sea coast. This area has been interpreted as a diapiric dome [Audren, 1987; 1990; Le Métour, 1978] or a Metamorphic Core Complex (MCC) [Brown and Dallmeyer, 1996]. However, the structural and radiometric data supporting these models are rare. This paper aims to present a microtectonic analysis of the newly defined here “Sarzeau Shear Zone” (SSZ) that will be interpreted as an extensional ductile shear zone. Moreover, monazite U-Th/Pb chemical datings of syn-kinematic leucogranite are also provided for the first time. The relationships between migmatites, plutonism and ductile shearing are discussed and replaced in the Late Carboniferous extensional framework of Southern Armorica.

GEOLOGICAL SETTING

The French Armorican Massif belongs to the European Variscan belt. It forms the northern part of the Ibero-Armorian orocline, a major syntaxis of the Variscan belt of Western Europe. The geodynamic evolution of the Armorican Massif is still discussed nevertheless most of authors agree with the following tectonic stages [e.g., Pin and Peucat, 1986; Ballèvre *et al.*, 1992; Matte, 2001; Faure *et al.*, 2005]. Since Early Ordovician, the Armorica microcontinent was rifted from the northern margin of Gondwana and the Medio-European (or Galicia–Central Massif) Ocean opened. This ocean closed in Late Silurian through a north-directed subduction. In Late Silurian or Early Devonian, the North-Gondwana margin, represented by the Southern part of the Armorican Massif and the entire Central Massif, experienced continental subduction responsible for nappe stacking and high-pressure metamorphism. This Eo-Variscan collision was followed in Early Devonian, around 390 Ma, by a pervasive crustal melting and the exhumation of the HP rocks [e.g. Cocherie *et al.*, 2005;

Faure *et al.*, 2008]. The Carboniferous evolution of the Armorican Massif is characterised by an intra-continental deformation coeval with granitic plutons emplacement.

The Armorican Massif is subdivided into several tectono-metamorphic domains by two dextral shear zones, namely the North Armorican Shear Zone (NASZ) and South Armorican shear zone (SASZ) that split into a WNW-ESZ northern branch and a NW-SE southern branch [Jégouzo, 1980] (fig.1b). However, these Carboniferous shear zones which developed late in the tectonic evolution do not represent suture zones or plate boundaries. When dealing with the Early Variscan collisional events, the Nort-sur-Erdre fault represents the suture zone (i.e. the remnant of the Medio-European Ocean) between Central Armorica (or Armorica microcontinent) and South Armorica. In the following, only an outline of South Armorica geology will be described, readers unfamiliar with the geology of the French Armorican Massif are referred to recent publication [e.g. Faure *et al.*, 2005].

South of the southern branch of the SASZ, several litho-tectonic units are described [e.g. Cogné, 1974; Le Corre *et al.*, 1991]. From top-to bottom, they are: i) the blueschist facies uppermost klippes of Ile de Groix and Bois de Cené, ii) the Upper Unit composed of intermediate pressure/temperature metamorphic rocks, iii) a Lower Unit made of high temperature metamorphic rocks and migmatites. Moreover, several generations of peraluminous plutons intrude the base of this nappe-stack (fig.1a).

In the study area, around the Golfe du Morbihan, only the later two units are recognised (fig.2a, b). There, the intermediate unit (Upper Unit), called the Vilaine and Belle Ile groups [Audren and Plaine, 1986] consists of metapelites, quartzites, or rare amphibolites and metarhyolites [Triboulet and Audren, 1988]. Structurally, these rocks, that belongs to the geometrically highest unit located to the SE and E of the Golfe du Morbihan are characterised by a sub-horizontal foliation and a NW-SE trending pervasive stretching lineation. The underlying unit consists of WNW-ESE trending sub-vertical to vertical migmatites that were

interpreted as a diapiric dome [Audren and Le Métour, 1976; Audren 1987; 1990] developed at the expense of paragneiss, orthogneiss, amphibolite and rare pyroxene bearing gneiss. These rocks are dated at 376 ± 19 Ma and 372 ± 24 Ma by whole rock Rb/Sr and zircon U/Pb methods, respectively [Pin and Peucat, 1986]. However, on the basis of recent monazite U-Th/Pb electron probe microanalyser (EPMA) analyses, these dates must be revised as Carboniferous (A. Cocherie, personal communication). North of Vannes, a biotite granite, called the S^{te}-Anne d'Auray massif develops widely (fig.2a, b). Meter to kilometre-scale bodies of the S^{te}-Anne d'Auray type granitic massif crop out within the migmatites foliation (fig.2a, b (cross section A)). Field and petrology observations show that the Golfe du Morbihan migmatites and the S^{te}-Anne d'Auray anatetic granite result from a same crustal-melting event. Moreover, the Golfe du Morbihan migmatites are intruded by numerous, NE-SW trending, fine-grained leucogranite dykes. The largest ones crop out in the Arradon cap or the Ile aux Moines (fig.2a, b cross section B). This granitic dyke swarm is collectively called “the Sarzeau granite” [Gapais *et al.*, 1993]. To the west of the study area crops out the Carnac granitic pluton (fig.2a) whose genetic relationships with the Sarzeau leucogranite will be discussed later.

West of the Golfe du Morbihan, the Quiberon Shear Zone is a kilometre-scale ductile extensional shear zone with top-to-the-W kinematics coeval with the emplacement of the Quiberon leucogranitic pluton. This shear zone has been interpreted as the structure responsible for the exhumation of the Golfe du Morbihan migmatites (fig.1a) [Gapais *et al.* 1993; Brown and Dallmeyer, 1996]. Yet, the systematic spatial association of ductile extensional shear zones and leucogranitic plutons in South Armorica has been generalised as a regional scale flat-lying detachment fault extending from Quiberon to the Sables d’Olonne in Vendée [Gapais *et al.*, 1993].

STRUCTURAL ANALYSIS

The “Golfe du Morbihan” experienced a polyphase tectono-metamorphic evolution as illustrated by several generations of ductile and brittle structures. The field-based structural analysis aims to 1) describe the first order structural framework of the study area, 2) define the main shear zone kinematics and 3) insure an accurate relation between structures and magmatic bodies.

I. Description of first-order structures

The major ductile structure, called the Sarzeau Shear Zone (SSZ hereafter), corresponds to the contact between the Upper and Lower Units (fig.2a, b). Furthermore, metre to decametre-scale low to moderately dipping faults and discrete ductile shear zones are scattered in the core of the Lower Unit. These discrete ductile shear bands are particularly concentrated near the top of the Lower unit. In the Lower Unit, low-strain domains preserve older structures. The 1/50 000 scale geological mapping (R. Augier, work in progress) allows us to accurately outline the SSZ. In map view, the SSZ shows a low to moderate angle of dip. It displays a 300 to 600m thick zone of S-C mylonites and locally ultramylonites (e.g. near Sarzeau village, fig.2a) embracing both the Upper Unit and the Lower Unit. However, strain is mostly concentrated in the footwall where mylonites reach locally 400m thick (fig.2a, b). Mylonites exhibit a sub-horizontal to gently (10° to 20°) eastward dipping foliation carrying a pervasive NW-SE trending stretching lineation often accompanied by unambiguous shear criteria.

Below the SSZ, scattered metre-scale shear bands and low-angle faults occur. The first ones are large-scale heterogeneities within the migmatites which foliation strikes about N 130° E with a vertical attitude. The best exposures are located on the cliffs at the Rohu cape (fg.3B and D). There, few decimetres to metre-scale shear zones concentrate into aplitic or pegmatitic dykes cutting across a migmatitic orthogneiss devoid of any post-migmatitic

ductile deformation (fig.3B and D). In the dykes, the deformation evolves from an S-C fabric to an ultramylonitic fabric from border to core, respectively (fig.3B).

Shear deformation is also accommodated by flat or gently dipping faults ranging from about 5 to 25° (fig.3E) that often overprint earlier ductile features; some of which are in their present geometry, gently dipping reverse faults (fig.4a). High-temperature striations, marked by quartz rods or fibres and preferred orientation of micas are often observed on low-angle fault planes. Quartz and muscovite crystallisations conspicuously present on these fault planes, argue for fluid circulation coeval with the faulting. The above described ductile structures are commonly reactivated during a late brittle stage of deformation as attested by cataclasitic zones and fault breccias. Generally, the ductile or ductile-brittle gently-dipping structures are reworked by highly-dipping faults (fig.3E).

II. SSZ kinematics

In the study area, a total of 52 structural sites, mainly located in the Lower Unit, were visited. A structural site is defined as a continuous outcrop of approximately 5 to 30m long, in which ductile structures and gently dipping fault planes can be observed. Distinction and sequence of ductile structures is the result of the confrontation of criteria such as (1) published pressure-temperature conditions of the deformation [i.e. Brown and Dallmeyer, 1996; Johnson and Brown, 2004], (2) cross-cutting field relations between successive deformational events and (3) reactivation of pre-existing defects.

At outcrop scale, the foliations and lineations have routinely been measured within the SSZ and at its vicinity. The sense of shear has been determined by well developed kinematic criteria such as S-C fabric, fold asymmetry or sigma or delta-type porphyroblast systems (fig.3C) [Paschier and Trouw, 1996]. The S-C fabric, particularly abundant in the Sarzeau granite, consistently indicates a top-to-the-SE shearing (fig.3A). In its present geometry, the

SSZ appears as an extensional shear zone with a top-to-the-SE kinematics. Meso-scale shear zones also display unambiguous kinematic indicators that also argue for a top-to-the-SE shearing in agreement with the SSZ (fig.3C).

Only the structural sites where ductile features such as shear bands (fig.3A) are not subsequently overprinted by brittle faults are presented in figure 4a. An average of 25 ductile shear planes and the associated lineation have been measured (Table 1) and plotted with the Tector software [Angelier, 1990] (fig.4a). The two-mica Sarzeau granite has been preferred as it is likely to be a material devoid of inherited structures. GPS locations as well as detail results are given in Table 1.

The lineation direction is well defined in most of structural sites and argue for a N 120°E stretching, the X finite strain axis over the study area. This stretching direction remains unchanged whatever the position of the sites along the strike of the SSZ. Nevertheless, it is worth to note that site 25 shows a rather N 177°E stretching that can be explained by a dextral rigid rotation around a vertical axis (fig.4a). Associated smaller-scale structures such as shear bands and low-angle faults (noted “S” on figure 4a) yield consistent N 120°E trending lineation associated with a top-to-the-SE sense of shear (fig.4a). Thus, the SSZ appears as a gently dipping extensional shear zone in its western part and admits in its eastern part a relative sinistral strike-slip motion (fig.2b, cross-section A), as shown in sites 21 and 42 (fig.4a). Therefore, the eastern part of the SSZ behaves as a transfer fault that accommodates the top-to-the-SE normal shearing. It is worth noting that a sinistral displacement along a NW-SE trending vertical fault is kinematically in contradiction with the dextral strike-slip displacement along the SASZ.

III. Typology and structure of the late granite dykes

As mentioned in the geological setting section, the Lower Unit is made of high-grade metamorphic rocks, migmatites and several generations of granitic bodies. The fine-grained two-mica Sarzeau granite is widespread in the study area, particularly within the SSZ where these rocks are deformed by a single set of shear bands (fig.2a, fig.4a). Field work in the SSZ footwall shows that the Sarzeau granite does not form a single pluton but rather consists of a dense network of meter-scale to kilometre-scale aplitic dykes (fig.2a, fig.4a). Two main types of dyke are recognised. The first one, which is volumetrically the most abundant, consists of isotropic fine-grained two-mica granite with sub-vertical sharp boundaries with respect to the surrounding rocks (fig.3F). The second type which is less abundant corresponds to systematically gently-west dipping dykes (i.e. 20 to 40°; fig.3G and H) showing sometimes a bending upward. The best exposures of this type of dyke are located in the western end of the Ile aux Moines (fig.2a). These dykes display an internal penetrative fabric defined by the alternation of quartz-feldspar-rich mica-poor, and biotite-rich layers lying parallel to the dyke borders which is interpreted here as a magmatic layering. Whatever their types the dykes cross-cut at right angle the host-rock migmatites (fig.3I and J).

The dyke preferred direction is clearly visible on the geological map (fig.2a, R. Augier work in progress, J. Le Métour work in progress). A statistical investigation, based on direct measurements of dyke walls, reveals an N 30°E regional consistency (fig.4b) that stands at right-angle from the NW-SE stretching direction inferred from the mineral lineation in the SSZ (fig.4a). It is worth noting that the eastern border of the Carnac pluton exhibits also several NNW-SSE trending apexes (fig.2a, J. Le Métour work in progress). On the basis of petrology and preliminary structural investigations, we propose that the Carnac pluton and the Sarzeau dyke swarm formed during the same magmatic event. The Carnac pluton might be considered as the feeder pluton of the Sarzeau dykes. Such an interpretation requires further

studies but seems to be in agreement with geological mapping and recent radiometric dating (A. Cocherie and J. Le Métour, personal communication).

TIME CONSTRAINTS

The EPMA is a very efficient tool for determining *in situ* ages. Due to the lack of common lead, and high U and Th contents, monazite is the most convenient mineral to apply the chemical U-Th/Pb geochronological method [Suzuki and Adachi, 1991; Cocherie and Albarède, 2001]. This method is suitable to determine the age of high temperature events such as magma crystallisation [e.g. Be *et al.*, 2006] or high temperature or fluid assisted recrystallisation. In this section, we aim to assign accurate time constraints on the S^{te}-Anne d'Auray type anatetic granite and two-mica Sarzeau granite.

I. Sampling strategy

Seven samples have been dated from the magmatic bodies of the Lower Unit of the Golfe du Morbihan area (see location in fig.2a and Table 2). Sample V.403 is from a S^{te}-Anne d'Auray type anatetic granite body interlayered within host-rocks migmatites. This rock V.403 consists in a biotite-rich granite where mylonitisation and metamorphic reactions are responsible for secondary muscovite blastesis coeval with progressive disappearance of biotite and grain-size reduction (quartz-feldspar grain size is about 0.5mm).

The other samples are from Sarzeau granite dykes intruding migmatites: samples V.102, V.104, V.108 and V.404 are undeformed granite picked structurally far below the SSZ (*ca* 800m to 3km). Conversely, samples V.402 and V.405 are from mylonitized granite within the SSZ exhibiting an averaged grain-size of about 0.3mm or even less. Petrologically, all these samples derive from above-mentioned quartz-plagioclase two-mica Sarzeau granite; the most deformed samples being devoid of biotite. The lack of biotite seems to be correlated to

an intense shearing as shown in figure 3A (V.405). All dated samples contain accessory-phases such as zircon, monazite, apatite and undifferentiated polymetallic oxides.

II. Analytical procedure

The analysed monazite grains were extracted by crushing and sieving of an average of 5 kilograms of rocks per sample, followed by heavy liquids separation by P. Jézéquel. For this study, the minerals were mounted in resin and polished. The monazite grains are then observed through a scanning electron microscope (SEM) in back-scattered electron (BSE) mode in order to choose the larger and less fractured grains for dating. The chemical analyses were carried out using a Cameca SX 50 EPMA operated jointly by the BRGM-CNRS - Orléans University. The accelerating-voltage and beam-current-intensity conditions were 20kV and 200nA, respectively. The counting time (peak, background) for monazite was 240s for Pb, 200s for U and 40s for all the other elements. According to this procedure, the detection limit (2σ) is 110ppm for Pb, 105ppm for U, and 130ppm for Th [Cocherie and Albarède, 2001]. The average grain U, Th and Pb contents are given in Table 2.

III. Monazite description

SEM-BSE observation allows us to recognise three monazite populations that are present in all dated samples. A representative grain for each population is shown in figure 5. The first population consists of grains with a patchy zoning related to a relatively large variation in Th and U contents (fig.5C). This kind of zoning is very common in monazite but does not reflect any growth zoning [Zhu and O’Nions, 1999, Cocherie *et al.*, 2005, Santosh *et al.*, 2006]. The second monazite population shows homogenous grains (fig.5A), and the third one represents zoned grains with a clear core and rim structure (fig.5B). This kind of zoning is characteristic

of a polyphase crystallisation [Be *et al.*, 2006]. All the grains selected for dating are unaltered and have a rather large size ranging from about 50 to 300 μm (Table 2).

IV. Results

Table 2 gives for each sample, the number of grains analysed, the number of analysis, the average size of the dated monazite, the Pb, U, Th contents, and Th/Pb and U/Pb ratios and the U-Th/Pb ages. The EPMA allows an age calculation from a small analytic spot (2 μm diameter) of U, Th and Pb concentrations. But, the multiplication of a large number of analyses in different grains from the same rock provides a statistical determination of an average age, assuming that all the analysed grains formed during the same stage of crystallisation. Details on the calculation method are given in Cocherie and Legendre (2007). Analytical data are plotted in a U/Pb vs. Th/Pb diagram [Cocherie and Albarède, 2001]. The statistical analysis and the graphic projection have been realised with the software EPMA dating.2 and Isoplot.3, respectively [Pommier *et al.*, 2002; Ludwig, 2004]. The rather large U concentrations (Table 2) and the significant variation in Th/U in the analysed monazite lead to a large spread of the data in the U/Pb vs. Th/Pb diagram. Consequently, a well-constrained regression line, close to the theoretical isochron can be defined (fig.6). Therefore, a statistical age can confidently be calculated at the centroid of the population. The theoretical Th-Pb and U-Pb ages calculated at the intercepts of the regression line with the axis are similar within the errors (fig.6), attesting to the quality of data processing.

To explore chemical and age significance of monazite core and rim zoning (fig.5B as a representative example), as discussed in Be *et al.* (2006), age scatter for a single monazite grain has been studied. Despite a large spread, the individual ages within cores and rims, plotted in figure 5d, yield statistically identical mean ages within uncertainty. All of the dated

core and rim zoned monazites yield internally consistent ages, irrespective of this chemical zoning, and argues for a single crystallisation event.

The S^{te}-Anne d'Auray type anatetic granite (Sample V.403) yields an age of 322 ±3Ma, (fig.6). Whatever their deformation state (i.e. mylonitised or not), the samples of Sarzeau granite give two age populations (fig.6) (i.e. Late Carboniferous and Late Devonian-Early Carboniferous). Samples V.402 and V.404 yield ages of 321 ±3Ma and 316 ±3Ma, respectively, which are similar within the errors. Conversely, samples V.104, V.108, and V.405 yield ages of 377 ±3Ma, 382 ±3Ma, and 379 ±4Ma respectively. Finally, sample V.102 gives an age of 365 ±3Ma. The geological significance of these Late Devonian-Early Carboniferous ages will be discussed in the next section.

DATA INTERPRETATION AND DISCUSSION

I. The Sarzeau granite as a strain and time marker for the extensional deformation

The field study highlighted that the Sarzeau granite consists in a dense network of fine-grained two-mica granite dykes. Preferred dyke orientations strikes N 30°E and then stands at right-angle with respect to the bulk N 120°E stretching deduced from the structural analysis. Based upon these geometric relations, it is then tempting to interpret this dyke population as tension gashes of various volumes coevally infilled by the Sarzeau granite. Traces of planar magmatic flow are the main characteristic of the second type of dyke. Furthermore this type of dyke with its upward bent geometry, suggest a progressive eastward shearing. Thus, the Sarzeau granite dykes are regarded as reliable strain markers consistent with the regional N 120°E stretching and deformed by the top-the-the-SE non-coaxial ductile shearing.

In high-strain zones where mylonites develop, dating the deformation is commonly achieved using the ⁴⁰Ar/³⁹Ar method on syn-kinematic micas [e.g. Muller *et al.*, 2001;

Sherlock *et al.*, 2003]. In this context, the $^{40}\text{Ar}/^{39}\text{Ar}$ age significance is dominantly controlled by recrystallisation processes rather than overall cooling [Agard *et al.*, 2002; Augier *et al.*, 2005]. Thus, the ages are interpreted to record the last increments of deformation. Commonly the early stages of deformation are overprinted and the duration of deformation remains poorly constrained. In our study, we are able to place constraints on the age of the early stage of deformation before mylonitic stage of the SSZ. The U-Th/Pb chemical method of monazite dating allows us to determine the age of granite emplacement [e.g. Be *et al.*, 2006; Cocherie *et al.*, 2005].

Monazites from the S^{te}-Anne d'Auray type anatectic granite yield an age of $322 \pm 3\text{ Ma}$ which is considered as representative for the partial-melting event responsible for the development of the Golfe du Morbihan migmatites and the S^{te}-Anne d'Auray pluton. It is noteworthy that this age complies with those obtained by the $^{207}\text{Pb}/^{206}\text{Pb}$ method on monazite [i.e. 323 ± 4 and $314 \pm 10\text{ Ma}$; Peucat, 1983]. Available ages for metamorphic peak-conditions are rare and controversial since they are based upon Rb/Sr whole rocks age ($379 \pm 19\text{ Ma}$) and U/Pb zircon populations ones ($381 \pm 10\text{ Ma}$ and $384 \pm 24\text{ Ma}$) [Vidal, 1980; Peucat, 1983].

Monazites from the Sarzeau granite dykes yield several distinctive age clusters: 316 ± 3 - $321 \pm 3\text{ Ma}$ and 377 ± 3 - $382 \pm 3\text{ Ma}$ ages and $365 \pm 3\text{ Ma}$ age. A straightforward conclusion is that the youngest age cluster will be considered as the Sarzeau granite emplacement age, in regard with field observation. The older ages are discussed below.

Comparison of the new monazite U-Th/Pb ages with available time-constraints is proposed in figure 7a. Closure temperatures for the different minerals and methods are given in the figure 7 caption. The last part of this chart could be divided in two steps of exhumation (from about 325 to 300Ma). Linear regression for the first segment, between *c.* $750 \pm 50^\circ\text{C}$ and $550 \pm 50^\circ\text{C}$ yield a cooling rate of the order of $11 \pm 2^\circ\text{C/Ma}$. A second step, during which exhumation from *c.* $550 \pm 50^\circ\text{C}$ to near surface conditions is achieved, is characterised by an

infinitely fast cooling rate due to the age clustering at *ca.* 300Ma. Because of the importance of error brackets for a given age and the sensitivity of closure temperature to various factors [Villa, 1998], an average cooling rate of $33 \pm 4^{\circ}\text{C} / \text{Ma}$ from $700 \pm 50^{\circ}\text{C}$ down to $85 \pm 50^{\circ}\text{C}$ can be computed. Whatever the possible exhumation paths (i.e. paths 1 and 2, figure 7a), our results point to fast cooling rates in agreement with Brown and Dallmeyer (1996) conclusions. Furthermore, these cooling rates are an order of magnitude faster than those expected for erosional processes [e.g. England and Thompson, 1984; Pinet and Souriau, 1988; Ring *et al.*, 1999 and enclosed references] and comparable to cooling rates obtained from various tectonic settings such as slab-retreat or lithosphere delamination [e.g. England and Thompson, 1984; Sonder *et al.*, 1987; Platt *et al.*, 1998; Augier *et al.*, 2005]. This result is well in line with published near-isothermal retrograde P-T path for the Golfe du Morbihan migmatites [Dallmeyer *et al.*, 1992; Brown and Dallmeyer, 1996] and the activity of major extensional shear zones roofing regionally the Lower Unit.

II. Significance of inherited ages within the Variscan framework

The ages of $377 \pm 3\text{Ma}$, $379 \pm 4\text{Ma}$ and $382 \pm 3\text{Ma}$, which are similar within the error and the 365 ± 3 Ma age, are obtained from monazite grains that are devoid of any evidence of recrystallisation or growth zoning. Therefore, these old ages can be interpreted as those of refractory grains inherited from earlier crystallisation stages during the Variscan orogeny.

Indeed, such Late Devonian to Early Carboniferous ages can be easily interpreted in the geological frame of the Variscan orogeny. The southern part of the Armorican Massif and the entire Central Massif belong to the internal zone of the Variscan Belt that experienced polyphase ductile and synmetamorphic deformation related to continental subduction of the North Gondwana margin below Armorica microcontinent. Several tectonic and metamorphic

events are responsible for the built up of the Southern Armorican Massif and Central Massif stack of nappes [e.g. Faure *et al.*, 2005 and enclosed references].

During Early to Middle Devonian, a D1 event is responsible for top-to-the-SW ductile shearing coeval with crustal melting and exhumation of the high-pressure rocks. In the Monts du Lyonnais, the migmatites yield a Rb/Sr whole rock age of 384 ± 16 Ma [Duthou *et al.*, 1994]. In the Limousin, the partial melting of orthogneiss has been dated at 375 ± 6 Ma, 383 ± 5 Ma, 378 ± 5 Ma by Rb/Sr whole rock, zircon U/Pb and monazite U-Th/Pb methods, respectively [Duthou, 1977; Lafon, 1986; Faure *et al.*, 2008]. Closer to the study area, the Champtoceaux migmatites, East of the SASZ, and south of Nort-sur-Erdre fault yield a monazite U-Th/Pb age of 387 ± 6 Ma [Cocherie *et al.*, 2005]. Moreover, migmatites from South Armorica yield a Rb/Sr whole rock and zircon U/Pb ages of 376 ± 19 Ma and 372 ± 24 Ma, respectively [Vidal, 1980; Peucat, 1983]. This D1 event is followed by a Late Devonian-Early Carboniferous D2 event coeval with an intermediate pressure-temperature metamorphism. At the end of the D2 event, per-aluminous biotite-cordierite plutons dated around 360-350 Ma, and called Guéret-type granitoids, emplaced in several places of the Central Massif [Berthier *et al.*, 1979; Cartannaz *et al.*, 2006; Faure *et al.*, 2008].

However, such magmatism event is not recognised in the southern part of the Armorican Massif. Nevertheless, it is reasonable to link up the two sets of inherited ages pointed out by our geochronological study with the tectonic, metamorphic and plutonic D1 and D2 events. The 377-380 Ma and 365 Ma monazite grains extracted from the Sarzeau granite could have crystallised during the D1 migmatisation or late D2 plutonism, respectively. Consequently, it might be argued that the Late Carboniferous Sarzeau granite formed by melting of underlying Early-Middle Devonian migmatites or Late Devonian-Early Carboniferous peraluminous granites.

In the Temperature-time plot (fig.7a), our Late Devonian-Early Carboniferous ages are in agreement with previous zircon U/Pb ones [Peucat, 1983]. These ages cluster in the high temperature field about 800°C-700°C. In the present state of knowledge, the link between these inherited Devonian ages and the Late Carboniferous cooling remains speculative (path 3, fig.7a). This straightforward path such as proposed by Brown and Dallmeyer (1996), although possible, is not documented yet; a two-stepped evolution stands as an alternative explanation (path 4, fig.7a).

III. Is the Lower Unit a metamorphic-core-complex?

Structural analyses conducted within the SSZ and on associated smaller-scale structures distributed toward the core of the Lower Unit show a consistently NW-SE oriented maximum principal finite strain axis and a top-to-the-SE sense of shear (fig.4a). The SSZ thus appears as a major extensional shear zone accommodating a top-to-the-SE normal shearing. Moreover, the ductile structures, particularly toward the top of the Lower Unit, display a clear reactivation under brittle conditions but with the same NW-SE maximum stretching direction (fig.3E, Turrillot work in progress). These kinematic patterns suggest that deformation is coeval with a bulk cooling when the Lower Unit reaches the surface [*ca.* 300Ma, Carpene *et al.*, 1979]. Our observations emphasize the synkinematic injection of the Sarzeau granite as tension gashes subsequently penetratively sheared within the SSZ.

It has been argued that the Lower Unit is a “metamorphic-core-complex” (MCC) [Brown and Dallmeyer, 1996]. However, MCC refers to a precise geometry and a peculiar behaviour of the continental crust [e.g. Davis and Coney, 1979; Crittenden *et al.*, 1980]. The syn-tectonic injection of Sarzeau and Quiberon granites and strain localisation along gently dipping ductile shear zones are in agreement with the MCC model. Nevertheless, two main points argue that the Golfe du Morbihan differs from a classical MCC as describe above.

Migmatites foliation is consistently vertical, and a dome shape cannot be documented. Furthermore, the SSZ cuts at right angle the migmatites foliation. These lines of evidence do not allow us to establish an unequivocal relationship between syn-plutonism extensional tectonics, anatexis and MCC development.

IV. Regional scale implications

Late-orogenic post-thickening thermal re-equilibration is often regarded as a key condition for large-scale pervasive extension and a way to exhume deeply buried metamorphic rocks [England and Thompson, 1984; Sonder *et al.*, 1987]. In South Armorica, a widespread Late-Carboniferous post-thickening extension characterised by crustal-scale extensional shear zones, migmatites domes and large amounts of granite has been described [Gapais *et al.*, 1993; Cagnard *et al.*, 2004]. In agreement with previous studies [Gapais *et al.*, 1993] our observations confirm that the Quiberon shear zone is a top-to-the-W mylonitic zone. The regional trend of the stretching lineation complies well with the interpretation of these extensional shear zones as orogen-parallel late-orogenic structures. Recently Cagnard *et al.* (2004) explored the different behaviour of the Variscan crust developed during and partly in response to late-orogenic extensional tectonics. Two “end-members” were defined. The first one is illustrated by the localised Quiberon extensional shear zone on which most of the strain is concentrated. The other one corresponds to a presumed migmatitic dome, such as the Sables d’Olonne area, which exhibits high thermal gradients of 70-80°C/km [Goujou, 1992] as well as a consistent flat-lying foliation. In this case, these observations therefore point to a pervasive crustal thinning at the roof of the migmatites [Cagnard *et al.*, 2004]. In the light of our new structural data the Golfe du Morbihan area is rather similar to the Quiberon model with strain localisation within the SSZ. However, the kinematics deduced from the Quiberon and Sarzeau shear zones, as well as the Sables d’Olonne area, are conflicting as they are top-

to-the-W (locally SW), to-the-SE and to-the-WNW respectively. Consequently, a single 200 km long detachment fault separating the Upper and Lower Units, as proposed by Gapais *et al.* (1993), can hardly account for the regional structure of southern Armorica. In contrast, it is therefore tempting to propose that late-orogenic extension was accommodated by a set of extensional structures, localised or not whose kinematics reflect local dynamics such as the inception of domes and granite bodies overprinted on the regional NW-SE crustal stretching.

CONCLUSION

The above reported new field structural investigation results, combined with the new monazite U-Th/Pb chemical dating from the Sarzeau two-mica granite allows us to constrain a part of the late-Variscan geodynamic evolution of the Golfe du Morbihan area. The extensional Sarzeau Shear Zone and the related ductile structures observed below both document a regional-scale N 120°E trending stretching coeval with emplacement of N 30°E trending leucogranitic dykes interpreted as kilometre-scale tension gashes. The monazite EPMA chemical dating yields a Late Carboniferous ages, *ca.* 316-321Ma for granite emplacement.

Crustal melting plays a major role in the late-orogenic exhumation of the ductile crust of southern Armorica. However, timing and detailed tectonic setting of the Golfe du Morbihan migmatites stay poorly documented as well as the late stage of their exhumation. Furthermore, the relationships between the belt-parallel extension and the dextral shearing along the South Armorican Shear Zone during the late-orogenic evolution of the Variscan belt remains unsettled yet.

Acknowledgements

This work was supported by the BRGM (CGF, French geological mapping programme) and the contribution of the ISTO (CNRS UMR 6113). We gratefully acknowledge P. Rossi A. Cocherie and J. Le Métour for fruitful discussions on geochronology and regional geology; P. Jézéquel for monazite extraction.

REFERENCES:

- AGARD P., MONIE P., JOLIVET L. & GOFFE B. (2002). - Exhumation of the Schistes Lustrés complex: in situ laser probe $^{40}\text{Ar}/^{39}\text{Ar}$ constraints and implications for the Western Alps. - *J. Metam. Geol.*, **20**, 599-618.
- ANGELIER J. (1990). - Inversion of field data in fault tectonics to obtain the regional stress-III. A new rapid direct inversion method by analytical means. - *Geophys. J. Intern.*, **103**, 363-376.
- AUDREN C. & LE METOUR J. (1976). – Mobilisation anatectique et déformation. Un exemple : les migmatites du Golfe du Morbihan (Bretagne Méridionale). - *Bull. Soc. Géol. France*, **4**, 1041-1049.
- AUDREN C. & PLAINE J. (1986)- Notice explicative. Carte géol. France (1/50 000), feuille Belle-Ile-en-Mer (447-477). Orléans, *Document BRGM*, 38p. Carte géologique par C. Audren, H. Hirbec, J. Plaine (1982).
- AUDREN C. (1987). - Evolution structurale de la Bretagne méridionale au Paléozoïque. - *Mémoire Soc. Géol. Minéral. Bretagne*, **31**, 365p.

AUDREN C. (1990). – Evolution tectonique et métamorphique de la chaîne Varisque en Bretagne méridionale. – *Schweizerische Mineralogische Petrographische Mitteilungen*, **70**, 17-34.

AUGIER R., JOLIVET L. & ROBIN C. (2005). - Late orogenic doming in the Eastern Betics : final exhumation of the Nevado-Filabride complex and its relation to basin genesis. - *Tectonics*, **24**, 19p.

BALLEVRE M., PARIS F. & ROBARDET M. (1992). – Corrélation ibero-armoricaines au Paléozoïque : une confrontation des données Paléobiogéographiques et tectonométamorphiques. - *C. R. Acad. Sci. Paris*, **315**, 1783-1789.

BE MEZEME E., COCHERIE A., FAURE M., LEGENDRE O. & ROSSI P. (2006). - Electron microprobe monazite geochronology of magmatic events: examples from Variscan migmatites and granitoids, Massif Central, France. – *Lithos*, **87**, 276–288.

BERTHIER F., DUTHOU J.-L. & ROQUES M. (1979). – Datation géochronologique Rb/Sr sur roches totales du granite de Guéret (Massif Central). Age fini-Dévonien de mise en place de l'un de ces faciès types. – *Bull. BRGM. Fr.*, **I**, 31-42

BROWN M. & DALLMEYER D. (1996). - Rapid Variscan exhumation and the role of magma in core complex formation: Southern Brittany Metamorphic Belt, France. - *J. Metam. Geol.*, **14**, 361-379.

BRUN J.-P. & BURG J.-P. (1982). – Combined thrusting and wrenching in the Ibero-Armorian arc: a corner effect during continental collision. – *Earth and Planetary Science Letters*, **61**, 319-332.

CAGNARD F., GAPAIS D., BRUN J.-P., GUMIAUX C. & VAN DEN DRIESCH J. (2004). - Late pervasive crustal-scale extension in the south Armorican Hercynian belt (Vendée, France). - *J. Struct. Geol.*, **26**, 435–449.

CARPENA J., CHAILLOU D., CHAMBAUDET A. & POUPEAU G. (1979). - Fission Track Geochronology of the Hercynian Platform in France. - *Report of the 10th International Conference on Solid State Nuclear Track Detectors*. Space Biophysics of the Parliament of the Council of Europe, Lyon.

CARTANNAZ C., ROLIN P., COCHERIE A., MARQUER D., LEGENDRE O., FANNING C.-M. & ROSSI P. (2006). – Characterisation of wrench tectonics from dating syn-to post-magmatism in the north-western French Massif Central. – *Int. J. Earth Sci.*, doi: 10.1007/s00531-006-0101-y.

CHERNIAK D.J.& WATSON E.B. (2000). - Pb diffusion in zircon. - *Chem. Geol.*, **172**, 5–24.

COCHERIE A. & ALBAREDE F. (2001). - An improved U-Th-Pb age calculation for electron microprobe dating of monazite. - *Geochim. Cosmochim. Acta*, **65**, 4509-4522.

COCHERIE A., BE MEZEME E., LEGENDRE O., FANNING C.M., FAURE M. & ROSSI P. (2005). – Electron microprobe dating as a tool for determining the closure of Th-U-Pb systems in migmatitic monazites. - *Am. Mineral.*, **90**, 607-618.

COCHERIE A. & LEGENDRE O. (2007). - Potential minerals for determining U-Th-Pb chemical age using electron microprobe. - *Lithos*, **93**, 288-309.

COGNE J. (1974). - Le Massif Armorican- In : DEBELMAS J., Eds., Géologie de la France, Doin, Paris, France, 105-161.

CRITTENDEN M.D., CONEY P.-J. & DAVIS G.H. (Eds.), (1980). - Cordilleran Metamorphic Core Complexes. - *Geological Society of America Memoir*, **153**.

DALLMEYER D., JOHANSSON L. & MOLLER C. (1992). - Chronology of Caledonian high-pressure granulite-facies metamorphism, uplift, and deformation within northern parts of the Western Gneiss Region, Norway. *Geological Society of America Memoir*, **104**, 444-455.

DAVIS G.H. & CONEY P.J. (1979). - Geological development of Cordilleran metamorphic core complexes. – *Geology*, **7**, 120–124.

DUTHOU J.-L. (1977). – Chronologie Rb-Sr et géochimie des granitoïdes d'un segment de la chaîne Varisque. Relation avec le métamorphisme : le Nord Limousin. – *Ann. Sci. Univ. Clermont-Ferrand*, **63**.

DUTHOU J.-L., CHENEVOY M. & GAY M. (1994). - Age Rb-Sr, Dévonien moyen des migmatites à cordiérite du Lyonnais (Massif central français). - *C. R. Acad. Sci. Paris*, **319**, 791-796.

ENGLAND P.-C. & THOMPSON A.-B. (1984). - Pressure-temperature-time paths of regional metamorphism, I. Heat transfer during the evolution of regions of thickened continental crust. - *Journal of Petrology*, **25**, 894-908.

FAURE M. & PONS J. (1991). – Crustal thinning recorded by the shape of the Namurian-Westphalian leucogranite in the Variscan Belt of the Northwest Massif Central, France. – *Geology*, **7**, 730-733.

FAURE M. (1995). - Late orogenic carboniferous extensions in the Variscan French Massif Central. - *Tectonics*, **14**, 132-153.

FAURE M., BE MEZEME E., DUGUET M., CARTIER C. LBOT & TALBOT J-Y. (2005). - Paleozoic tectonic evolution of medio-Europa from the example of the French Massif Central and Massif Armorican. - In: CAROSI R., DIAS R., IACOPINI D. & ROSENBAUM G., Eds., The southern Variscan belt, *J. of the Virtual Explorer*, Electronic Edition, ISSN 1441-8142, **19**, Paper 5. Site web <http://virtualexplorer.com.au>.

FAURE M., BE MEZEME E., COCHERIE A., ROSSI P., CHEMENDA A. & BOUTELIER D. (2008). – Devonian geodynamic evolution of the Variscan Belt, insights from the French Massif Central and Massif Armorican. – *Tectonics*, (in press).

GAPAIS D., LAGARDE J.-L., LE CORRE C., AUDREN C., JEGOUZO P., CASAS SAINZ A. & VAN DEN DRIESCH J. (1993). - La zone de cisaillement de Quiberon: témoin d'extension de la chaîne Varisque en Bretagne méridionale au Carbonifère. - *C. R. Acad. Sci. Paris*, **316**, 1123–1129.

GOUJOU J.-C. (1992). - Analyse pétro-structurale dans un avant-pays métamorphique: influence du plutonisme tardi-orogénique Varisque sur l'encaissant épi à mésozonal de Vendée. – *Document BRGM*, **216**.

GUNNELL Y. & LOUCHET A. (2000). - The influence of rock hardness and divergent weathering on the interpretation of apatite fission-track denudation rates - Evidence from charnockites in South India and Sri Lanka. - *Zeitschrift für Geomorphologie*, **44**, 33–57.

JEGOUZO P. (1980). – The South Armorican Shear Zone. – *J. Struct. Geol.*, **2**, 39-47.

JENKIN G.R.T., ELLAM R.M., ROGERS G. & STUART F.M. (2001). - An investigation of closure temperature of the biotite Rb-Sr system: The importance of cation exchange. - *Geochim. Cosmochim. Acta*, **65**, 1141-1160.

JOHNSON T. & BROWN M. (2004). - Quantitative Constraints on Metamorphism in the Variscides of Southern Brittany - a Complementary Pseudosection Approach. - *Journal of Petrology*, **45**, 1237-1259; doi:10.1093/petrology/ehg012.

JOLY A., CHEN Y., FAURE M. & MARTELET G. (2007). - A multidisciplinary study of a syntectonic pluton close to a major lithospheric-scale fault: relationships between the

Montmarault granitic massif and the Sillon Houiller Fault in the Variscan French Massif Central. Part I: Geochronology, mineral fabrics and tectonic implications. - *J. Geophys. Res.*, **112**, B10104, <http://dx.doi.org/10.1029/2006JB004745>.

KAGAMI H., SHIMURA T., YUHARA M., OWADA M., OSANAI Y. & SHIRAISHI K. (2003). - Resetting and closing condition of Rb-Sr whole-rock isochron system: some samples of metamorphic and granitic rocks from the Gondwana super-continent and Japan Arc. - *Polar Geosci.*, **16**, 227-242.

KAMBER B. S., FREI R. & GIBB A. J. (1998). - Pitfalls and new approaches in granulite chronometry. An example from the Limpopo Belt, Zimbabwe. - *Precambrian Research*, **91**, 269–285.

KRETZ R. (1983). - Symbols of rock forming minerals. - *Am. Mineral*, **68**, 277-279.

LAFON J.M. (1986). - Géochronologie U-Pb appliquée à deux segments du Massif Central Français. Le Rouergue oriental et le Limousin central. - 152 p., *Thèse d'Etat, Univ. Montpellier*.

LE CORRE C., AUVRAY B., BALLEVRE M. & ROBARDET M. (1991). - Le massif Armorique. - In: PIQUE A., Eds., Massifs anciens de France. *Sci. Géol. Strasbourg*, 31-103.

LE METOUR J. (1978). – Petrogenesis of migmatites and associated granites in South Brittany. – *N. Jb. Miner. Mh.*, **8**, 364-376.

LUDWIG K.R. (2004). - User's manual for ISOPLOT/EX, version2. A geochronological toolkit for Microsoft Excel (version 3.1). – *Berkeley Geochronology Center Spec. Publ.* **1a**, 43 p.

MALAVIEILLE J., GUIHOT P., COSTA S., LARDEAUX J.M. & GARDIEN V. (1990). - Collapse of the thickened Variscan crust in the French Massif Central: Mont Pilat extensional shear zone and St Etienne upper Carboniferous basin. - *Tectonophysics*, **177**, 139-149.

MATTE P. (2001). - The Variscan collage and orogeny (480-290 Ma) and the tectonic definition of the Armorica microplate: a review. - *Terra Nova*, **13**, 122-128.

MULLER W., KELLEY S. & VILLA I. M. (2001). - Dating fault-generated pseudotachylytes: comparison of $^{40}\text{Ar}/^{39}\text{Ar}$ stepwise-heating, laser ablation and Rb-Sr micro-sampling analysis. - *Contributions to Mineralogy and Petrology*, **144**, 57-77.

PASSCHIER C. W. & TROUW R. A. J. (1996). – Microtectonics. – In :SPRINGER-VERLAG, Eds., Berlin, 289 p.

PEUCAT J.-J. (1983). - Géochronologie des roches métamorphiques (Rb-Sr et U-Pb). Exemples choisis au Groenland, en Laponie, dans le Massif armoricain et en Grande Kabylie. - *Mém. Soc. Géol. Minéral Bretagne*, **28**, 158p.

PIN C. & PEUCAT J.-J. (1986). - Age des épisodes de métamorphisme paléozoïques dans le Massif central et le Massif armoricain. - *Bull. Soc. Géol. France*, **8**, 461-469.

PINET P. & SOURIAU M. (1988). – Continental erosion and large scale relief. – *Tectonics*, **7**, 553-582.

PLATT J.-P., SOTO J.I., WHITEHOUSE M.J., HURFORD A.J. & KELLEY S.P. (1998). – Thermal evolution, rate of exhumation, and tectonic signification of metamorphic rocks from the floor of the Alboran extensional basin, western Mediterranean. – *Tectonics*, **17**, 671-689.

POMMIER A., COCHERIE A. & LEGENDRE O. (2002). - EPMA Dating User's manual: Age calculation from electron probe microanalyser measurements of U-Th-Pb. *Document BRGM*, 9 p.

RING U., BRANDON M.T., WILLETT S.D. & LISTER G.S. (1999). – Exhumation processes. – In: RING U., BRANDON M.T., WILLETT S.D. & LISTER G.S., Eds., Exhumation processes: normal faulting, ductile flow and erosion. *Geological Society Special Publication*, 1-27.

ROIG J.Y., FAURE M. & TRUFFERT C. (1998). - Folding and granite emplacement inferred from structural, strain, TEM, and gravimetric analyses : the case study of the Tulle antiform, SW French Massif Central. - *J. Struct. Geol.*, **20**, 1169-1189.

SANTOSH M., COLLINS A.S., TAMASHIRO I., KOSHIMOTO S., TSUTSUMI Y. & YOKOYAMA K. (2006). – The timing of ultrahigh-temperature metamorphism in Southern India: U-Th-Pb electron microprobe ages from zircon and monazite in sapphirine-bearing granulites. – *Gondwana Research*, **10**, 128-155.

SONDER L.-J., ENGLAND P.C., WERNICKE B.P. & CHRISTIANSEN, R.L. (1987). - A physical model for Cenozoic extension of western North America. In: COWARD R.J., DEWEY J.F., HANCOCK P.L., Eds., Continental Extensional Tectonics. *Geological Society Special Publication*, **28**, 187–201.

SHERLOCK S.C, KELLEY S.P., ZALASIEWICZ J.A., SCHOFIELD D.I., EVANS J.A., MERRIMAN R.J. & KEMP S. J. (2003). - A new approach to dating slate: Ar-Ar Laser probe analysis of strain fringes in the Welsh Basin slate belt, UK. - *J. Geophys. Res.*, **5**, 219-222.

SUZUKI K. & ADACHI M. (1991). - The chemical Th-U-total Pb isochron ages of zircon and monazite from the gray granite of the Hida terrane, Japan. - *J. Earth Sci. Nagoya Univ.*, **38**, 11-37.

TALBOT J.-Y., CHEN Y. & FAURE M. (2005). - Pluton-dykes relationships from AMS and microstructural studies in a Variscan granite from French Massif Central. - *J. Geophys. Res.*, **110**, B12106, doi:10.1029/2005JB003699.

TRIBOULET C. & AUDREN C. (1988). - Controls on P-T-t-deformation path from amphibole zonation during progressive metamorphism of basic rocks (estuary of the river Vilaine, south Brittany, France). - *J. Metam. Geol.*, **6**, 117-133.

VAN DEN DRISSCHE J. & BRUN J.-P. (1991-92). - Tectonic evolution of the Montagne Noire (French Massif Central) : a model of extensional gneiss dome. - *Geodinamica Acta*, **5**, 85-99.

VIDAL P. (1980). - L'évolution polyorogénique du Massif Armorican : apport de la géochronologie et de la géochimie isotopique du strontium. - *Mém. Soc. Géol. Minéral. Bretagne*, **21**, 162p.

VILLA I.M. (1998). - Isotopic closure. - *Terra Nova*, **10**, 42–47.

ZHU X. K. & O'NIONS R. K. (1999). – Zonation of monazite in metamorphic rocks and its implication for high temperature thermochronology: a case study from the Lewisian terrain. - *Earth and Planetary Science Letters*, **171**, 209-220.

FIGURE CAPTIONS:

Fig.1 - Geological overview of the Armorican Massif and South Armorica [modified from Cagnard *et al.*, 2004]. (a) Simplified map of the entire Armorican Massif. Shown are three main tectonic domains of the Armorican Massif: North Armorica, Central and South Armorica. NASZ: North Armorican Shear Zone; SASZ: South Armorican Shear Zone; N-sur-EF: Nort-sur-Erdre fault; (b) Close-up view of the South Armorica. Are represented the main units and the associated tectonic features.

Fig.1 - Aperçu géologique du Massif Armoricain et du domaine Sud Armoricain [modifié d'après Cagnard et al., 2004]. (a) Carte géologique simplifiée du Massif Armoricain dans son intégralité. Le massif Armoricain est présenté avec ses trois principaux domaines tectoniques : Nord, Centre et Sud Armoricaine. NASZ : Zone de Cisaillement Nord Armoricain; SASZ : Zone de Cisaillement Sud Armoricain; N-sur-EF est la faille de Nort-sur-Erdre; (b) Vue détaillée du domaine Sud Armoricain avec ses principales unités constitutives et les structures tectoniques qui les séparent.

Fig.2 - (a) Geological map of the Golfe du Morbihan study area, showing the main tectonostratigraphic units and their internal features. Shown are Central Armorica to the NE; To the SW, the upper and the lower tectonic units separated by late-orogenic extensional Sarzeau shear zone. White stars indicate the emplacement of samples for monazite U-Th/Pb dating switch. White polygons locate outcrops and hand-samples pictures displayed in figure 3; (b) Interpretative cross section through the study area (noted A and B on map (a)). The legend of the main formations and structures for both map and cross section are the same.

Fig.2 - (a) Carte géologique de la région du Golfe du Morbihan (zone d'étude) montrant les principales unités tectoniques et leur structure interne. Le domaine Centre Armorican affleure au NE de la carte ; les unités supérieures et inférieures du domaine Sud-Armorican sont séparées par la zone de cisaillement extensive tardio-orogénique de Sarzeau. Les étoiles blanches indiquent la position des échantillons (avec leur nom) ayant été datés par la méthode U-Th/Pb. Les polygones blancs localisent la position des affleurements et des échantillons pris en photo et présentés sur la figure 3; (b) Coupes géologiques interprétatives

au travers de la zone d'étude (notée A et B sur la carte (a)). La légende est commune à la carte et aux coupes.

Fig.3 - Representative microphotographs and outcrop pictures of ductile structures and their relationships with the main magmatic bodies (i.e. S^{te}-Anne d'Auray type, Carnac and Sarzeau granites) and the surrounding high-grade migmatites. Pictures are located by the white polygons in figure 2. (A) Picture of a cut and polished hand-sample of S-C mylonites derived from the Sarzeau two-mica granite within the SSZ. These mylonites are routinely 300 to 600 meters-thick. Sense of shear is consistently top-to-the-SE (see fig.4); (B) Second-order shear zone (i.e. satellite shear zone) located in a fine-grained dyke of anatetic S^{te}-Anne d'Auray type granite which is then intensively sheared and mylonitized; (C) Thin section of ultramylonite from the previous outcrop (picture B). This section shows consistent shear sense indicators; note the δ-type mantled porphyroblast of K-feldspar (at the top of the section) in a quartz-feldspar-mica ultramylonitic matrix; (D) Outcrop-scale picture taken a few tens of meters West (=below) from the previous one. Mylonitic fine-grained anatetic granite dyke displays clear cross-cutting relationships with respects to the Ordovician host-rocks (orthogneiss). This dyke, as the previous one (picture B), displays a top-to-the-SE sense of shear; (E) Flat to gently E-dipping small-scale shear zone carrying a well-developed N 120°E mineral lineation and high-temperature striations (see explanations in text) in a large-scale two-mica Sarzeau granite dyke. This ductile shear zone is offset by high angle normal faults; (F) Structural relationships between a steeply dipping N30°E-striking two-mica Sarzeau granite dyke (“type 1”, see text for explanations) and the surrounding migmatites that underwent a polyphased tectonometamorphic evolution. Inset (I) is a close-up view of the sharp contact between the migmatites and the dykes; (G) Gently dipping (“type 2”, see text

for explanations) two-mica Sarzeau granite dyke striking N30°E. The dyke presents an internal magmatic layering parallel to the dyke wall. Inset (J) shows the same cross cutting relationships between the migmatites and the dyke; (H) Picture taken at right angle from the picture G to appreciate the geometrical relations between the surrounding migmatites and the “type 2” dykes.

Fig.3 - *Photographies d'affleurements et de lame mince montrant quelques exemples représentatifs d'objets déformés, ainsi que leurs relations avec les principaux corps magmatiques de la zone d'étude (granites de type S^{te}-Anne d'Auray de Carnac et de Sarzeau) et les roches métamorphiques de haut-grade environnantes (migmatites). Ces photos sont localisées sur la carte de la figure 2 par les polygones blancs.* (A) Détail d'un échantillon coupé et poli de mylonites S-C de granite de Sarzeau provenant de la Zone de Cisaillement de Sarzeau (SSZ). Cette zone de cisaillement a une épaisseur structurale de 300 à 600 mètres. Le sens de cisaillement déduit de l'analyse de ces mylonites est systématiquement vers le SE. (voir figure 4) ; (B) Bande de cisaillement de second-ordre (dite satellite) localisée dans un filon de granite de type S^{te}-Anne d'Auray qui est alors fortement cisallé et mylonitisé ; (C) Photographie d'une lame mince d'ultramylonite échantillonnée sur l'affleurement précédent (photo B). L'analyse de la déformation, dont la structure d'enroulement du porphyroblaste de feldspath est un exemple de critère (en haut de la lame), révèle un cisaillement vers le SE ; (D) Photographie d'un affleurement situé à quelques dizaines de mètres à l'Ouest du précédent. Un filon mylonitisé de granite anatectique à grain fin recoupe clairement la foliation verticale de l'encaissant orthogneissique (orthogneiss ordovicien). Ce filon, comme le précédent (B) montre des critères de cisaillement vers le SE ; (E) Bande de cisaillement dans un large filon de granite de Sarzeau, localisée, plate à légèrement pentée vers l'E portant une linéation minérale bien développée ainsi que des stries de haute température

orientée N120°E. Cette bande de cisaillement est réactivée et décalée par des failles normales à fort angle; (F) Relations géométriques entre un filon à fort pendage de granite de Sarzeau à deux micas orienté N30°E (filon de “type 1”, voir les explications dans le texte) et les migmatites encaissantes qui ont subi une évolution tectonométamorphique complexe. L’encart (I) est une vue rapprochée du contact entre les migmatites et le filon; (G) Photographie d’un filon faiblement penté de “type 2” (voir explications dans le texte) de granite de Sarzeau de direction N30°E. Ce filon présente un litage magmatique interne parallèle à ses épontes. L’encart (J) montre les relations de recouplement perpendiculaires entre la foliation migmatitique et le filon; (H) Photographie prise à 90° de la précédente pour apprécier les relations géométriques entre les migmatites et le filon de “type 2”.

Fig.4 - (a) Geological map restricted to the SSZ. Are located on the map, the 16 tectonic stations where structural analyses have been done within and away from the SSZ (the latter are noted “S” for second-order shear zones). Solid black arrows indicate the strike of the stretching lineation and the associated sense of shear. Structural measurements (S-plane or C-plane and associated lineation) were plotted with the Tector software in lower hemisphere projection [Angelier, 1990]. Are also represented, for some tectonic sites the average stretching lineation direction carried by the foliation planes (solid lines). In the most deformed tectonic sites (especially within the SSZ) the lineation carried by S planes is overprinted by penetrative shear planes, such as in ultramylonite bodies (fig.3C for example); (b) Preferred direction of the Sarzeau dykes (67 measurements).

Fig.4 - (a) carte géologique limitée au tracé de la SSZ. Localisation des 16 stations où ont été réalisées les mesures structurales dans et loin de la SSZ (ces derniers sites sont notés “S”

(pour déformation de second-ordre). Les flèches noires massives indiquent l'orientation de la linéation d'étirement ainsi que le sens de cisaillement associé. Les mesures structurales (plans S ou plans C ainsi que la linéation qu'ils portent) ont été projetées en hémisphère inférieur avec le programme Tector [Angelier, 1990]. La direction moyenne de la linéation portée par les plans de foliation est également représentée par la ligne noire épaisse; sur les sites les plus déformés, particulièrement dans la SSZ, celle-ci est effacée (photographies C de la fig.3 par exemple); (b) Directions préférentielles des filons de granite de Sarzeau (67 mesures).

Fig.5 - SEM BSE pictures showing representative internal structure of monazite grains from dated samples (A, B and C). (A) Monazite showing an homogenous texture; (B) Monazite showing a core and rim zonation. This kind of zoning is normally due to a two-stage crystallisation. White dots represent the position of the chemical analysis made with the microprobe analyser; (C) Monazite showing a patchy zoning whose chemical significance is not clearly established; (D) Representation of all apparent ages yielded from the monazite M23 grain (from sample V.404; rim as well as core ages), plotted in an average age diagram. Explanations are given in the text.

Fig.5 - Image au Microscope Electronique à Balayage (MEB) en électrons rétrodiffusés montrant les textures internes des populations de monazite des échantillons (A, B et C). (A) Monazite montrant une texture interne homogène; (B) Monazite montrant une zonation de type « cœur-bordure ». Ce type de zonation est normalement issu d'une cristallisation en deux étapes. Les points blancs sont les positions des analyses chimiques ponctuelles réalisées à la microsonde; (C) Monazite montrant une zonation de type « patchy zoning » dont la

signification n'est pas clairement établie; (D) Représentation de tous les âges provenant des analyses réalisées sur le grain de monazite M23 (échantillon V.404) tant sur le cœur que la bordure, projetés dans un diagramme de type âges moyens. Les explications sont données dans le texte.

Fig.6 - U/Pb vs. Th/Pb isochron diagrams. All standard deviations are quoted at 95% confidence level and error ellipses are plotted as 2σ . Are given on each diagram the name and the magmatic body (S^{te}-Anne d'Auray type anatetic and two-mica Sarzeau granites), the number of analyzed monazite grain, the isochron calculated age, the number of analysis (n) and the value of the MSWD parameter; (a) The significance of the lines is given on a theoretical chart at the bottom-right of the figure.

Fig.6 - Diagrammes isochrones U/Pb vs. Th/Pb. Les erreurs sont établies avec un degré de confiance de 95% et les ellipses d'erreur avec une incertitude à 2σ . A chaque diagramme y est associé le nom de l'échantillon ainsi que le nom du corps magmatique dans lequel il a été prélevé (granites anatectique de type S^{te}-Anne d'Auray et granite de Sarzeau), le nombre de grains de monazite analysés, l'âge isochrone calculé, le nombre d'analyses (n) et la valeur du paramètre statistique MSWD ; (a) La signification des courbes et des lignes constitutives de ces diagrammes est donnée sur un diagramme théorique et fictif en bas à droite de la figure.

Fig.7 - (a) Temperature-time (T-t) plot for the Golfe du Morbihan migmatites, the S^{te}-Anne d'Auray type anatetic granite and the two-mica Sarzeau granite (belonging to the Lower Unit see fig.2) based upon a compilation of available ages: whole-rock (WR) ages and on minerals

ages such as zircon (Zrn), monazite (Mnz), hornblende (Hbl), biotite (Bt), muscovite (Ms) and apatite (Ap) [mineral abbreviations from Kretz, 1983]. References origins of ages are yielded on the figure. Solid grey lines and dotted line (4) represent a new interpretative T-t path for Golfe du Morbihan segment of South Armorica from about 400Ma to 280Ma. The dotted line (3) represents a segment of the T-t path (from about 400Ma to 330Ma) proposed by Brown and Dallmeyer (1996). The lines (1) and (2) represent possible exhumation paths for the period from about 325 to 300Ma. Mineral ages and their estimated closure temperature (CT) are shown with errors brackets. CT for the different methods used are: monazite, $^{206}\text{Pb}/^{207}\text{Pb}$, *c.* $800 \pm 50^\circ\text{C}$ [Kamber *et al.*, 1998]; monazite, U-Th/Pb, *c.* $700 \pm 50^\circ\text{C}$ [Cocherie *et al.*, 2005]; U-Pb zircon, *c.* $800 \pm 50^\circ\text{C}$ [Cherniak and Watson 2000]; RT, Rb/Sr, *c.* $700 \pm 50^\circ\text{C}$ [Kagami *et al.*, 2003]; biotite, Rb/Sr, *c.* $325 \pm 25^\circ\text{C}$ [Jenkin *et al.*, 2001]; muscovite, Ar/Ar, *c.* $425 \pm 50^\circ\text{C}$ [Villa, 1998]; hornblende, Ar/Ar, *c.* $550 \pm 50^\circ\text{C}$ [Villa, 1998]; and apatite, fission-tracks (FT) *c.* $85 \pm 25^\circ\text{C}$ [Gunnell, 2000]. (b) WNW-ESE representative orogen-parallel cross-section through the Quiberon and the Golfe du Morbihan area. Main tectono-metamorphic subdivisions are presented with the same legend and formalism than in figure 4a.

Fig.7 - (a) Diagramme Température-temps (T-t) pour les migmatites du Golfe du Morbihan, le granite anatectique de type S^{te}-Anne d'Auray et le granite de Sarzeau (Unité Inférieure, voir fig.2), basé sur une compilation des âges disponibles dans la littérature. Ceux-ci sont constitués d'un âge roche-totale (WR) et d'âges sur minéraux comme le zircon (Zrn), la monazite (Mnz), la hornblende (Hbl), la biotite (Bt), la muscovite (Ms) and l'apatite (Ap) [abréviations minérales selon Kretz, 1983]. Les références à l'origine des âges reportés sont données directement sur la figure. Les courbes enveloppes grises reliées par la courbe pointillée (4) sont une proposition de chemins T-t (depuis 400Ma jusque vers 280Ma) qu'adoptent les roches de l'Unité Inférieure du Golfe du Morbihan. La ligne pointillée (3)

présente un segment du chemin $T-t$ (depuis 400Ma jusque vers 330Ma) proposé par Brown et Dallmeyer (1996). Les lignes (1) et (2) présentent deux types d'exhumation possible pour la période allant de 325 à 300Ma environ. Les âges ainsi que les températures de fermeture présumées (CT) sont présentées avec leurs barres d'erreur respectives. Les CT des différentes méthodes utilisées sont: monazite, $^{206}Pb/^{207}Pb$, $800 \pm 50^\circ C$ [Kamber et al., 1998]; monazite, U-Th/Pb, $700 \pm 50^\circ C$ [Cocherie et al., 2005]; U-Pb zircon, $800 \pm 50^\circ C$ [Cherniak and Watson 2000]; RT, Rb/Sr, $700 \pm 50^\circ C$ [Kagami et al., 2003]; biotite, Rb/S, $325 \pm 25^\circ C$ [Jenkin et al., 2001]; muscovite, Ar/Ar, $425 \pm 50^\circ C$ [Villa, 1998]; hornblende, Ar/Ar, $550 \pm 50^\circ C$ [Villa, 1998]; and apatite, Traces de Fission (FT) $85 \pm 25^\circ C$ [Gunnell, 2000]. (b) Coupe WNW-ESE, parallèle à l'orogène au travers des régions de Quiberon et du Golfe du Morbihan. Les principales subdivisions tectono-métamorphiques sont présentées avec le même formalisme que sur la figure 4a.

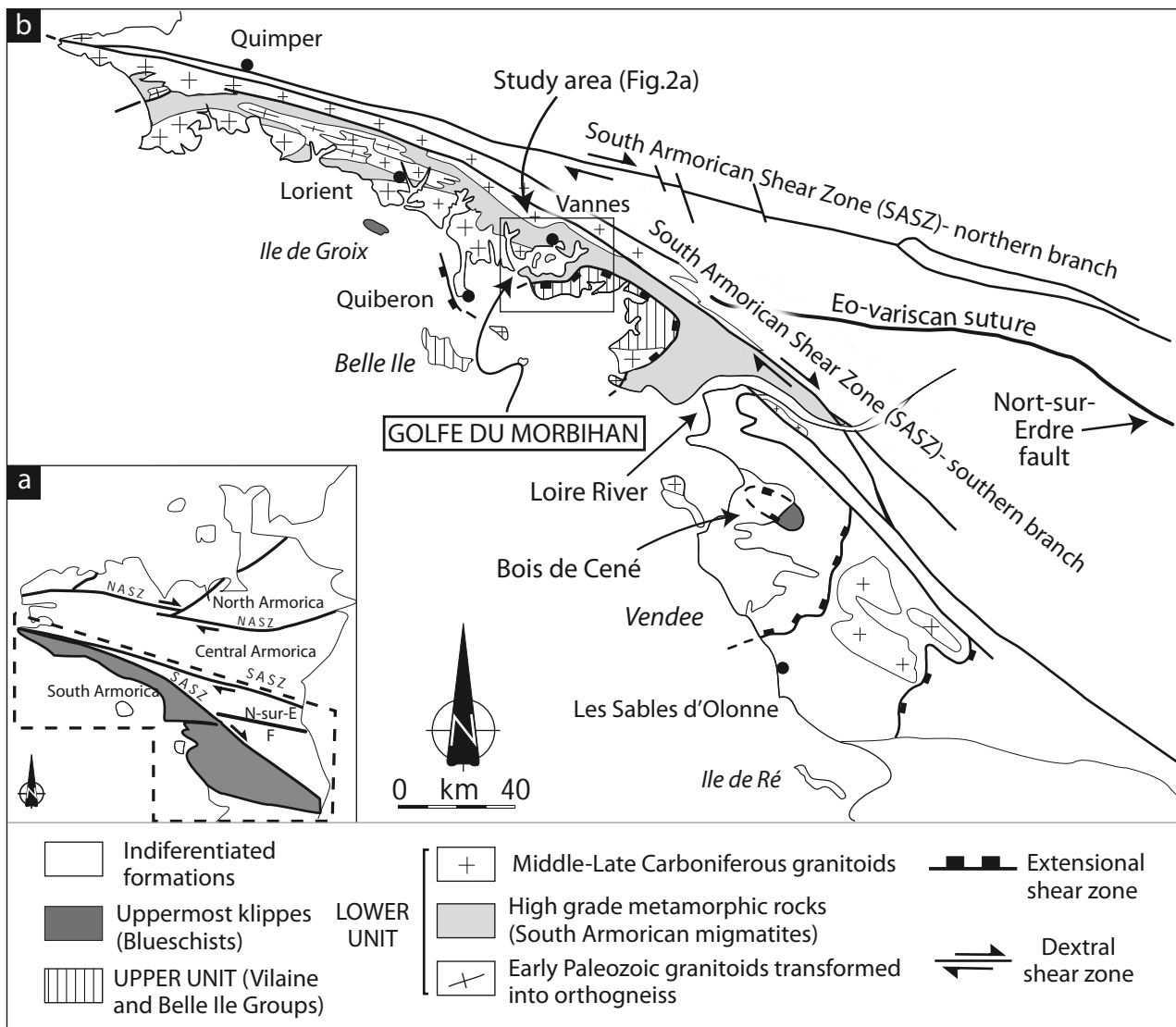


Fig. 1

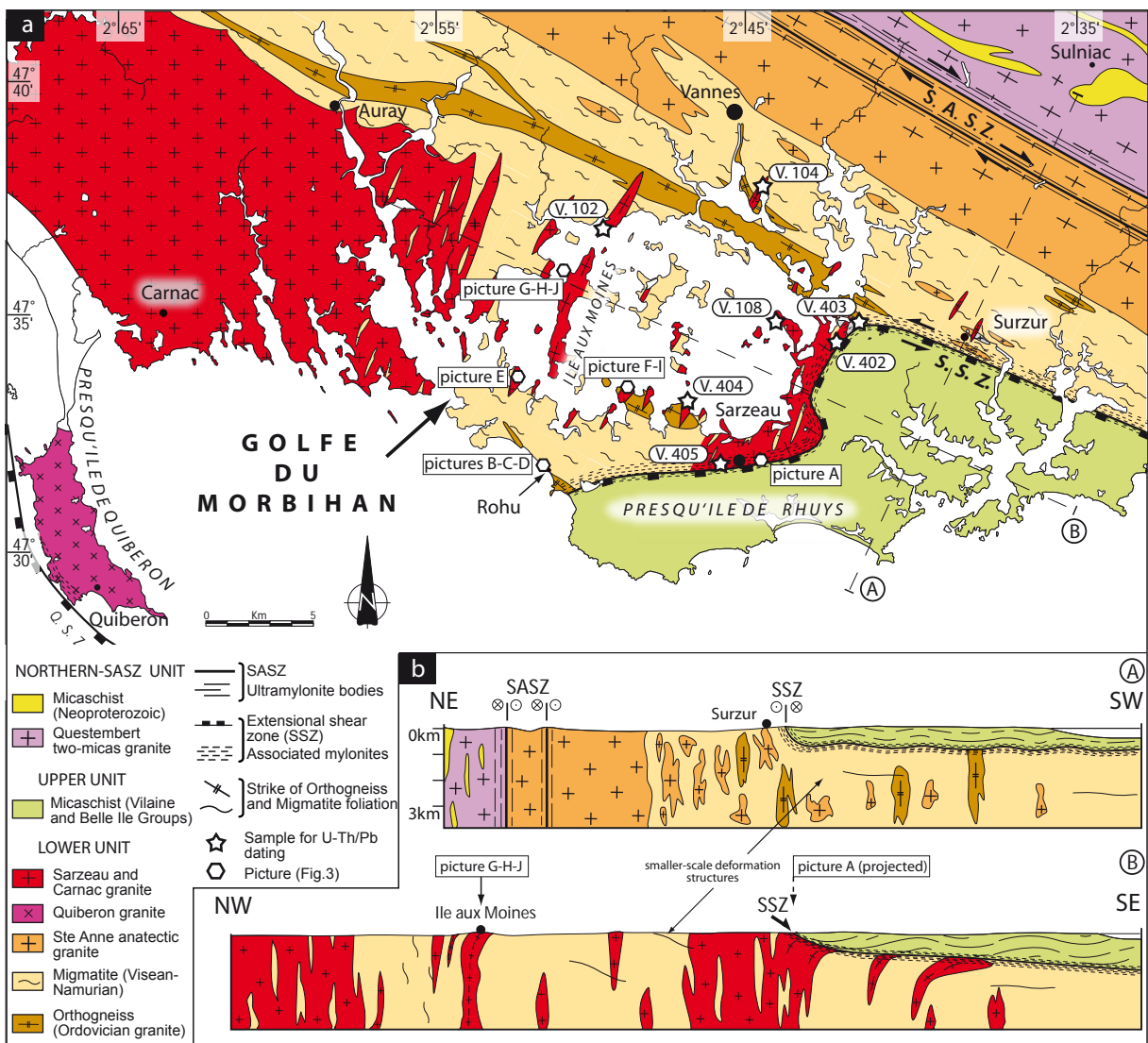


Fig.2

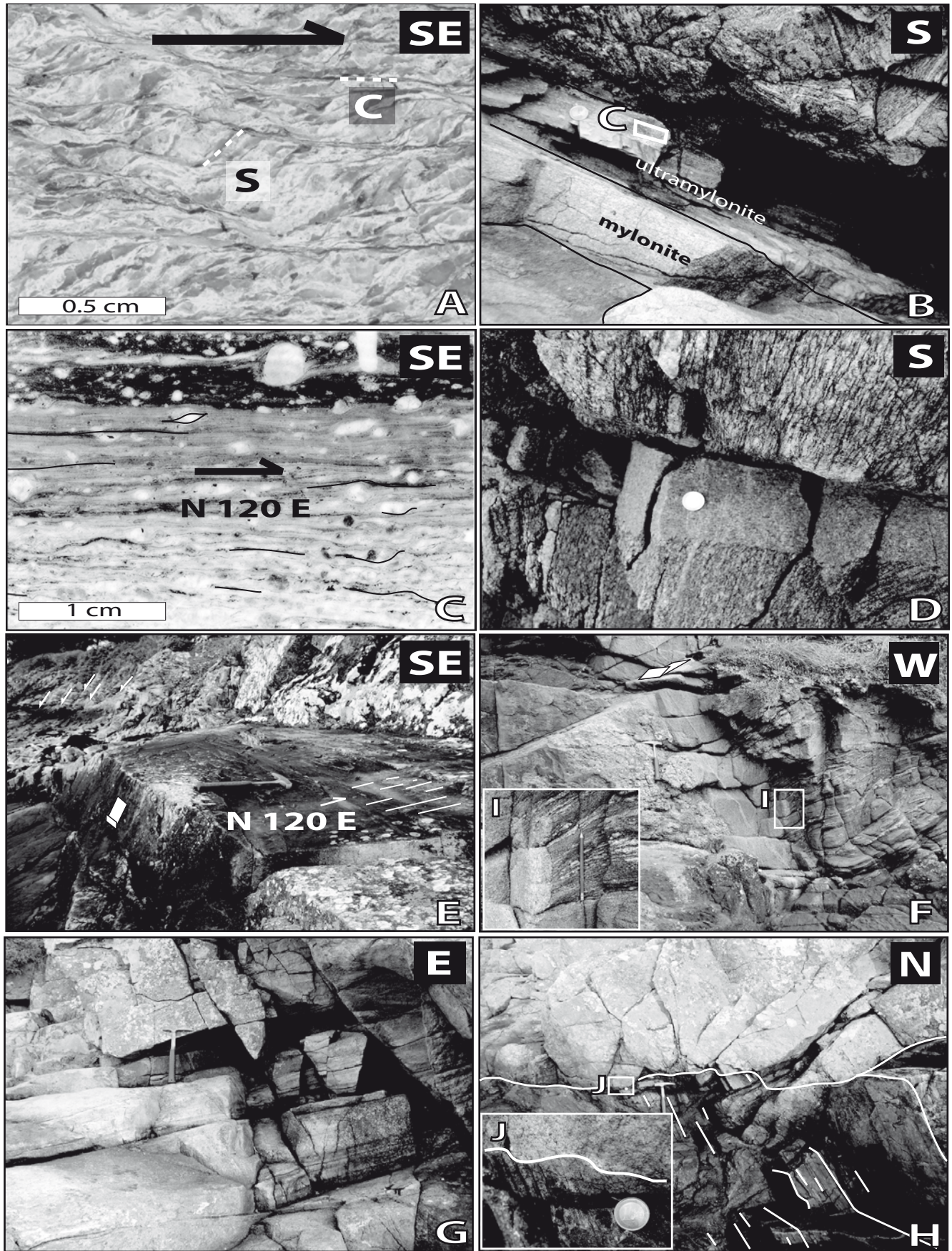


Fig.3

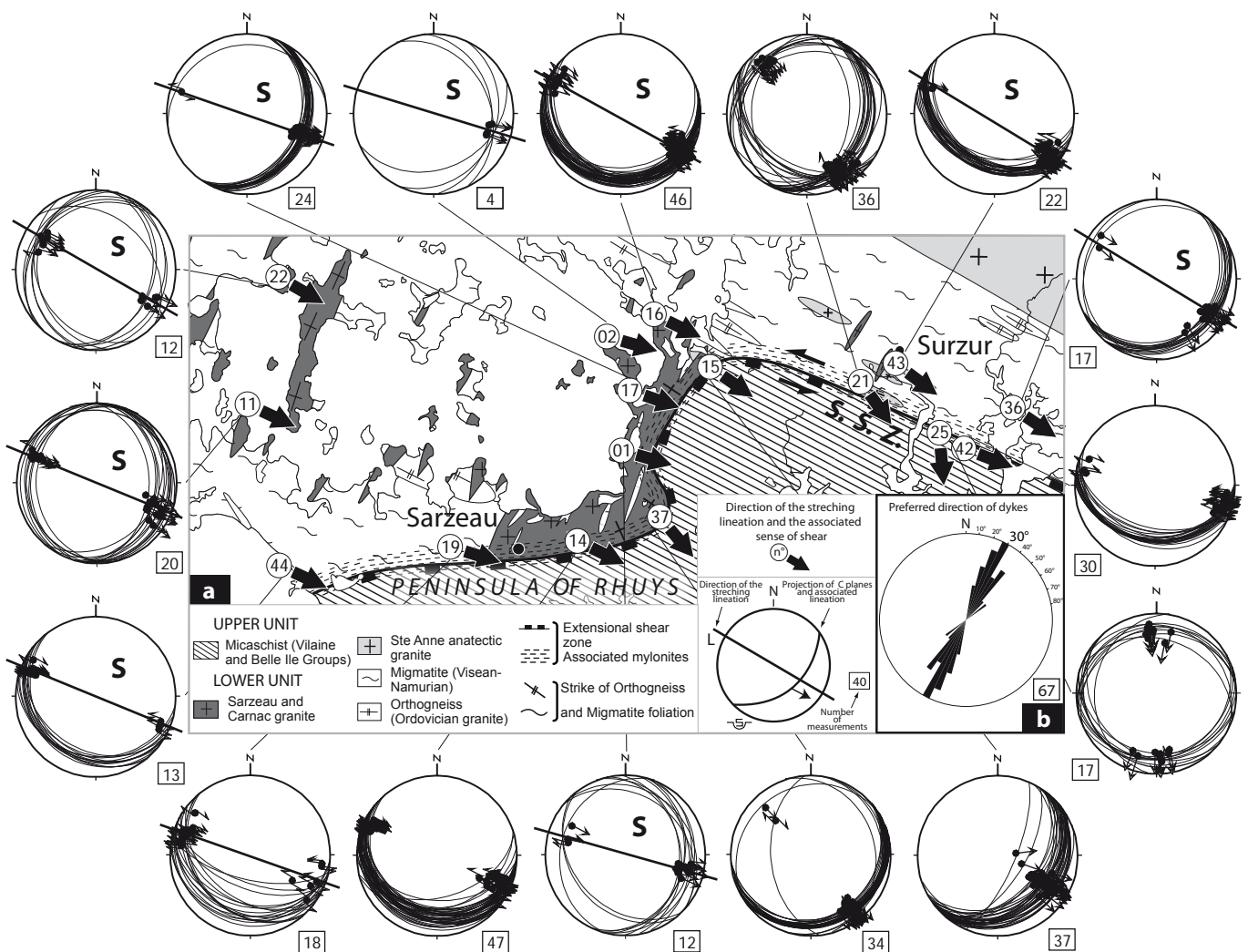


Fig.4